

# Characterization of Production GaAs Solar Cells for Space

B. E. Anspaugh

December 15, 1988



National Aeronautics and  
Space Administration

Jet Propulsion Laboratory  
California Institute of Technology  
Pasadena, California

(NASA-CR-1848(3) CHARACTERIZATION OF  
PRODUCTION GaAs SOLAR CELLS FOR SPACE (Jet  
Propulsion Lab.) 37 p U.S. GPO: 1988-10A

N89-20549

Unclas  
G3/44 0198854

1. Report No. 88-39	2. Government Accession No.	3. Recipient's Catalog No.	
4. Title and Subtitle CHARACTERIZATION OF PRODUCTION GaAs SOLAR CELLS FOR SPACE		5. Report Date December 15, 1988	
		6. Performing Organization Code	
7. Author(s) B.E. Anspaugh		8. Performing Organization Report No.	
9. Performing Organization Name and Address JET PROPULSION LABORATORY California Institute of Technology 4800 Oak Grove Drive Pasadena, California 91109		10. Work Unit No.	
		11. Contract or Grant No. NAS7-918	
		13. Type of Report and Period Covered JPL Publication	
12. Sponsoring Agency Name and Address NATIONAL AERONAUTICS AND SPACE ADMINISTRATION Washington, D.C. 20546		14. Sponsoring Agency Code	
15. Supplementary Notes			
16. Abstract <p>The electrical performance of GaAs solar cells was characterized as a function of irradiation with protons and electrons with the underlying goal of producing solar cells suitable for use in space. Proton energies used varied between 50 keV and 10 MeV, and damage coefficients were derived for liquid phase epitaxy GaAs solar cells. Electron energies varied between 0.7 and 2.4 MeV.</p> <p>Cells from recent production runs were characterized as a function of electron and proton irradiation. These same cells were also characterized as a function of solar intensity and operating temperature, both before and after the electron irradiations.</p> <p>The long term stability of GaAs cells during photon exposure was examined. Some cells were found to degrade with photon exposure and some did not. Calibration standards were made for GaAs/Ge solar cells by flight on a high altitude balloon.</p>			
17. Key Words (Selected by Author(s)) Conversion Techniques Power Sources		18. Distribution Statement Unclassified--Unlimited	
19. Security Classif. (of this report) Unclassified	20. Security Classif. (of this page) Unclassified	21. No. of Pages 30	22. Price

JPL Publication 88-39

# Characterization of Production GaAs Solar Cells for Space

B. E. Anspaugh

December 15, 1988



National Aeronautics and  
Space Administration

Jet Propulsion Laboratory  
California Institute of Technology  
Pasadena, California

The research described in this publication was carried out by the Jet Propulsion Laboratory, California Institute of Technology, and was sponsored by the Air Force Wright Aeronautical Laboratories through an agreement with the National Aeronautics and Space Administration.

Reference herein to any specific commercial product, process, or service by trade name, trademark, manufacturer, or otherwise, does not constitute or imply its endorsement by the United States Government or the Jet Propulsion Laboratory, California Institute of Technology.

## ABSTRACT

The electrical performance of GaAs solar cells was characterized as a function of irradiation with protons and electrons with the underlying goal of producing solar cells suitable for use in space. Proton energies used varied between 50 keV and 10 MeV, and damage coefficients were derived for liquid phase epitaxy GaAs solar cells. Electron energies varied between 0.7 and 2.4 MeV.

Cells from recent production runs were characterized as a function of electron and proton irradiation. These same cells were also characterized as a function of solar intensity and operating temperature, both before and after the electron irradiations.

The long term stability of GaAs cells during photon exposure was examined. Some cells were found to degrade with photon exposure and some did not. Calibration standards were made for GaAs/Ge solar cells by flight on a high altitude balloon.

CONTENTS

INTRODUCTION . . . . . 1  
PROCEDURES . . . . . 2  
REFERENCES . . . . . 5  
APPENDIX . . . . . 26

Figures

Figure 1.  $I_{SC}$  vs 1 MeV Electron Fluence for Three Types of GaAs Solar  
Cells . . . . . 12  
Figure 2. Normalized  $I_{SC}$  vs 1 MeV Electron Fluence for Three Types of  
GaAs Solar Cells . . . . . 13  
Figure 3.  $V_{OC}$  vs 1 MeV Electron Fluence for Three Types of GaAs Solar  
Cells . . . . . 14  
Figure 4. Normalized  $V_{OC}$  vs 1 MeV Electron Fluence for Three Types of  
GaAs Solar Cells . . . . . 15  
Figure 5.  $I_{mp}$  vs 1 MeV Electron Fluence for Three Types of GaAs Solar  
Cells . . . . . 16  
Figure 6. Normalized  $I_{mp}$  vs 1 MeV Electron Fluence for Three Types of  
GaAs Solar Cells . . . . . 17  
Figure 7.  $V_{mp}$  vs 1 MeV Electron Fluence for Three Types of GaAs Solar  
Cells . . . . . 18  
Figure 8. Normalized  $V_{mp}$  vs 1 MeV Electron Fluence for Three Types of  
GaAs Solar Cells . . . . . 19

Figure 9. $P_{\max}$ vs 1 MeV Electron Fluence for Three Types of GaAs Solar Cells . . . . .	20
Figure 10. Normalized $P_{\max}$ vs 1 MeV Electron Fluence for Three Types of GaAs Solar Cells . . . . .	21
Figure 11. $I_{\text{SC}}$ vs Intensity at 28°C for GaAs/Ge Solar Cells . . . . .	22
Figure 12. $V_{\text{OC}}$ vs Temperature at 135.3 mW/cm <sup>2</sup> for GaAs/Ge Solar Cells . .	23
Figure 13. $P_{\max}$ vs Intensity at 28°C for GaAs/Ge Solar Cells . . . . .	24
Figure 14. $P_{\max}$ vs Temperature at 135.3 mW/cm <sup>2</sup> for GaAs/Ge Solar Cells .	25

Tables

Table 1. Average Short-Circuit Current: Pre-Irradiation . . . . .	6
Table 2. Average Open-Circuit Voltage: Pre-Irradiation . . . . .	6
Table 3. Average Maximum Power: Pre-Irradiation . . . . .	7
Table 4. Average Fill Factor: Pre-Irradiation . . . . .	7
Table 5. Average Short-Circuit Current: After 1 x 10 <sup>15</sup> e/cm <sup>2</sup> . . . . .	8
Table 6. Average Open-Circuit Voltage: After 1 x 10 <sup>15</sup> e/cm <sup>2</sup> . . . . .	8
Table 7. Average Maximum Power: After 1 x 10 <sup>15</sup> e/cm <sup>2</sup> . . . . .	9
Table 8. Average Fill Factor: After 1 x 10 <sup>15</sup> e/cm <sup>2</sup> . . . . .	9
Table 9. Average Short-Circuit Current: After 1 x 10 <sup>16</sup> e/cm <sup>2</sup> . . . . .	10
Table 10. Average Open-Circuit Voltage: After 1 x 10 <sup>16</sup> e/cm <sup>2</sup> . . . . .	10
Table 11. Average Maximum Power: After 1 x 10 <sup>16</sup> e/cm <sup>2</sup> . . . . .	11
Table 12. Average Fill Factor: After 1 x 10 <sup>16</sup> e/cm <sup>2</sup> . . . . .	11

## CHARACTERIZATION OF PRODUCTION GaAs SOLAR CELLS FOR SPACE

### INTRODUCTION

This publication is the final report of a contract between Air Force Wright Aeronautical Laboratories and Jet Propulsion Laboratory. The objective of the contract was to evaluate GaAs solar cells for space as they evolved from the prototype stage into cells manufactured on a production line. The GaAs cells were characterized electrically as a function of electron and proton irradiation. During the course of the contract, several hundred cells were irradiated with protons from the Caltech accelerators using energies between 50 keV and 10 MeV, and with electrons from the JPL Dynamitron accelerator with energies of 0.7, 1.0, and 2.4 MeV. The proton irradiation work on early liquid phase epitaxy cells made by Hughes Research Lab was reported in Refs. 1 and 2.

An additional task was assigned to this project when it was found that some GaAs cells appeared to degrade when exposed to light beams for long periods of time. Accordingly, the scope of the contract was expanded and several experiments were carried out to try to identify whether the problem was real, what was causing the degradation, and, if possible, identify a cure. A second add-on task was completed in the summer of 1988 when two calibration standards made of GaAs/Ge cells were flown on the annual JPL solar cell calibration balloon flight. The calibrations were performed and the cells were shipped to the sponsor in October, 1988. A description of the balloon calibration flight and the results of the 1988 flight are reported in Ref. 3.

This report consists of two parts. The first part is a writeup of our most recent measurements of GaAs/Ge solar cells under electron irradiation. The latter cells were irradiated with 1 MeV electrons with a schedule of fluences out to  $1 \times 10^{16}$  e/cm<sup>2</sup>. The electrical characteristics of these cells were also measured as a function of temperature and intensity before irradiation, after  $1 \times 10^{15}$  e/cm<sup>2</sup>, and after  $1 \times 10^{16}$  e/cm<sup>2</sup>. These characteristics were measured at an experimental matrix of temperatures and intensities which included temperatures of -20, 28, 60, 100, and 140 °C, and intensities of 50, 100, 135.3, and 250 mW/cm<sup>2</sup>. The second part is a report on the photon degradation work, given here as a copy of a paper which was presented at the 20th IEEE Photovoltaic Specialists Conference in September, 1988, (Ref. 4 included as the Appendix in this publication).

#### PROCEDURES

The GaAs/Ge solar cells were received at JPL in May, 1988 and the measurements were made in September and October, 1988. Fifteen cells were irradiated and the electrical characteristics of those 15 cells are plotted in Figures 1 through 10. Included in these plots for comparison are plots of the radiation behavior of two earlier types of GaAs solar cells. A summary of the three cell types in these plots is as follows:

<u>Mfg</u>	<u>Cell Type</u>	<u>Window Depth</u>	<u>Jcn. Depth</u>	<u>Vintage</u>
HRL	LPE GaAs/GaAs	0.2 μm	0.35 μm	1984
ASEC	OMCVD Early Mantech	0.1 μm	0.45 μm	1984
ASEC	OMCVD GaAs/Ge	0.08μm	0.50 μm	1988

All cells are 2 x 2 cm<sup>2</sup>.

Of the 15 GaAs/Ge cells which were irradiated, 5 were also subjected to the matrix of temperature/intensity measurements described above. After the

appropriate fluences had been administered, these 5 cells were mounted in a special vacuum chamber designed to perform solar cell measurements at various controlled temperatures and intensities. The cells are illuminated through a 7940 fused silica window using a Spectrolab X-25 solar simulator as the illumination source. The cells are each held down onto a temperature controlled block with a pair of spring clamps. One clamp is positioned on the busbar of the cell so that it also serves as the electrical contact for the top of the cell. The other applies pressure on the front surface of the cell, on the opposite side from the first clamp. Its purpose is to apply pressure to force the cell tightly against the temperature controlled block and balance the pressure exerted by the contact clamp. As a consequence, the clamp shades approximately  $0.036 \text{ cm}^2$  of the cell area, which is approximately 0.9% of the area of a 2 x 2 cm cell. The data reported here have not been corrected for this shading. Indium foil (5 mils thick) is placed between the cells and the thermal plate in order to achieve good thermal contact. The simulator intensity incident on the cells in the chamber is set by using a balloon flown calibration cell inside the chamber. The temperature of this standard cell is independently controlled and maintained at  $28^\circ \text{ C}$  throughout the test. The current-voltage (I-V) electrical data is measured by a computer based data acquisition system. The results are plotted as I-V curves and the important parameters are printed in digital form.

Statistical analysis is also provided by the data acquisition program in the form of averages and standard deviations of the cell electrical parameters. The data from the temperature/intensity parametric measurements are presented in tabular form in Tables 1 through 12. Each entry in these tables is a 5 cell average. Some representative plots of solar cell

parameters as a function of either temperature or intensity (with fluence as parameter) are presented in Figures 11 through 14. The symbols on each Figure are five cell averages of the solar cell parameter, and the straight lines are linear least squares fits to the data. An inset box in each Figure shows the slopes of the calculated least squares fits.

#### REFERENCES

1. B. E. Anspaugh and R. G. Downing, "Radiation Effects in Silicon and Gallium Arsenide Solar Cells Using Isotropic and Normally Incident Radiation," JPL Publication 84-61, Jet Propulsion Laboratory, Pasadena, CA, Sept. 1984.
2. B. E. Anspaugh and R. G. Downing, "Radiation Effects in Silicon and Gallium Arsenide Solar Cells Using Isotropic and Normally Incident Radiation," Conf. Record of the 17th IEEE Photovoltaic Specialists Conf., 23, 1984.
3. B. E. Anspaugh and R. S. Weiss, "Results of the 1988 NASA/JPL Balloon Flight Solar Cell Calibration Program," JPL Publication 88-36, Jet Propulsion Laboratory, Pasadena, CA, November 1, 1988.
4. Bruce Anspaugh, Ram Kachare and Peter Iles, "Photon Degradation of AlGaAs/GaAs Solar Cells," to be published in Conf. Record of the 20th IEEE Photovoltaic Specialists Conf., 1988 (included as the Appendix in this publication).

Table 1. Average Short-Circuit Current: Pre-Irradiation

ASEC GaAs/Ge Solar Cells  
 AlGaAs Window Depth: 0.08  $\mu$   
 Junction Depth: 0.50  $\mu$   
 Buffer Layer: 6-9  $\mu$   
 2 x 2 cm x 225  $\mu$   
 Dual AR Coating  
 Sample Size 5 TM-91

Cell Temp. ( °C )	Solar Intensity (mW/cm <sup>2</sup> )			
	<u>50</u>	<u>100</u>	<u>135.3</u>	<u>250</u>
-20	42.5	83.4	113.5	207.6
28	43.9	85.9	116.9	214.8
60	44.6	89.5	121.9	220.8
100	46.4	94.4	126.3	227.1
140	47.7	96.0	130.5	233.2

Table 2. Average Open-Circuit Voltage: Pre-Irradiation

ASEC GaAs/Ge Solar Cells  
 AlGaAs Window Depth: 0.08  $\mu$   
 Junction Depth: 0.50  $\mu$   
 Buffer Layer: 6-9  $\mu$   
 2 x 2 cm x 225  $\mu$   
 Dual AR Coating  
 Sample Size 5 TM-91

Cell Temp. ( °C )	Solar Intensity (mW/cm <sup>2</sup> )			
	<u>50</u>	<u>100</u>	<u>135.3</u>	<u>250</u>
-20	1112.9	1187.3	1206.7	1202.8
28	1000.8	1058.9	1075.3	1077.0
60	910.3	960.1	976.6	990.4
100	794.8	838.7	853.6	877.4
140	703.1	740.1	754.5	780.5

Table 3. Average Maximum Power: Pre-Irradiation

ASEC GaAs/Ge Solar Cells  
 AlGaAs Window Depth: 0.08  $\mu$   
 Junction Depth: 0.50  $\mu$   
 Buffer Layer: 6-9  $\mu$   
 2 x 2 cm x 225  $\mu$   
 Dual AR Coating  
 Sample Size 5 TM-91

Cell Temp. ( °C )	Solar Intensity (mW/cm <sup>2</sup> )			
	<u>50</u>	<u>100</u>	<u>135.3</u>	<u>250</u>
-20	32.08	66.06	96.57	174.14
28	30.40	62.03	85.62	156.93
60	28.31	59.61	82.58	151.16
100	25.92	56.30	76.88	140.96
140	23.13	49.83	66.68	126.25

Table 4. Average Fill Factor: Pre-Irradiation

ASEC GaAs/Ge Solar Cells  
 AlGaAs Window Depth: 0.08  $\mu$   
 Junction Depth: 0.50  $\mu$   
 Buffer Layer: 6-9  $\mu$   
 2 x 2 cm x 225  $\mu$   
 Dual AR Coating  
 Sample Size 5 TM-91

Cell Temp. ( °C )	Solar Intensity (mW/cm <sup>2</sup> )			
	<u>50</u>	<u>100</u>	<u>135.3</u>	<u>250</u>
-20	0.681	0.670	0.656	0.662
28	0.693	0.683	0.682	0.679
60	0.698	0.694	0.694	0.692
100	0.703	0.711	0.713	0.707
140	0.691	0.701	0.677	0.694

Table 5. Average Short-Circuit Current: After  $1 \times 10^{15} \text{ e/cm}^2$

ASEC GaAs/Ge Solar Cells  
 AlGaAs Window Depth:  $0.08 \mu$   
 Junction Depth:  $0.50 \mu$   
 Buffer Layer:  $6-9 \mu$   
 $2 \times 2 \text{ cm} \times 225 \mu$   
 Dual AR Coating  
 Sample Size 5 TM-91

Cell Temp. ( °C )	Solar Intensity ( $\text{mW/cm}^2$ )			
	<u>50</u>	<u>100</u>	<u>135.3</u>	<u>250</u>
-20	34.9	69.1	94.2	174.4
28	36.4	72.2	98.7	179.7
60	37.4	75.3	102.4	185.2
100	38.8	77.3	106.1	189.3
140	40.6	80.4	109.2	198.3

Table 6. Average Open-Circuit Voltage: After  $1 \times 10^{15} \text{ e/cm}^2$

ASEC GaAs/Ge Solar Cells  
 AlGaAs Window Depth:  $0.08 \mu$   
 Junction Depth:  $0.50 \mu$   
 Buffer Layer:  $6-9 \mu$   
 $2 \times 2 \text{ cm} \times 225 \mu$   
 Dual AR Coating  
 Sample Size 5 TM-91

Cell Temp. ( °C )	Solar Intensity ( $\text{mW/cm}^2$ )			
	<u>50</u>	<u>100</u>	<u>135.3</u>	<u>250</u>
-20	1064.6	1131.5	1149.5	1150.5
28	938.5	990.6	1007.6	1017.3
60	840.9	888.7	908.1	929.1
100	723.8	765.5	783.2	810.0
140	631.3	668.5	684.5	712.3

Table 7. Average Maximum Power: After  $1 \times 10^{15} \text{ e/cm}^2$

ASEC GaAs/Ge Solar Cells  
 AlGaAs Window Depth:  $0.08 \mu$   
 Junction Depth:  $0.50 \mu$   
 Buffer Layer:  $6-9 \mu$   
 $2 \times 2 \text{ cm} \times 225 \mu$   
 Dual AR Coating  
 Sample Size 5 TM-91

Cell Temp. ( °C )	Solar Intensity ( $\text{mW/cm}^2$ )			
	<u>50</u>	<u>100</u>	<u>135.3</u>	<u>250</u>
-20	25.62	54.07	74.70	136.32
28	23.40	49.54	68.78	124.68
60	21.58	46.17	64.34	117.90
100	19.31	41.20	58.06	105.83
140	17.08	36.65	51.21	95.76

Table 8. Average Fill Factor: After  $1 \times 10^{15} \text{ e/cm}^2$

ASEC GaAs/Ge Solar Cells  
 AlGaAs Window Depth:  $0.08 \mu$   
 Junction Depth:  $0.50 \mu$   
 Buffer Layer:  $6-9 \mu$   
 $2 \times 2 \text{ cm} \times 225 \mu$   
 Dual AR Coating  
 Sample Size 5 TM-91

Cell Temp. ( °C )	Solar Intensity ( $\text{mW/cm}^2$ )			
	<u>50</u>	<u>100</u>	<u>135.3</u>	<u>250</u>
-20	0.690	0.694	0.692	0.681
28	0.685	0.694	0.693	0.683
60	0.687	0.691	0.692	0.686
100	0.687	0.697	0.699	0.691
140	0.667	0.682	0.685	0.678

Table 9. Average Short-Circuit Current: After  $1 \times 10^{16} \text{ e/cm}^2$

ASEC GaAs/Ge Solar Cells  
 AlGaAs Window Depth:  $0.08 \mu$   
 Junction Depth:  $0.50 \mu$   
 Buffer Layer:  $6-9 \mu$   
 $2 \times 2 \text{ cm} \times 225 \mu$   
 Dual AR Coating  
 Sample Size 5 TM-91

Cell Temp. ( $^{\circ}\text{C}$ )	Solar Intensity ( $\text{mW/cm}^2$ )			
	<u>50</u>	<u>100</u>	<u>135.3</u>	<u>250</u>
-20	23.1	46.0	62.6	115.5
28	24.4	48.5	66.3	121.2
60	25.2	50.3	69.1	124.9
100	26.5	53.4	72.4	131.6
140	27.9	56.1	76.4	139.0

Table 10. Average Open-Circuit Voltage: After  $1 \times 10^{16} \text{ e/cm}^2$

ASEC GaAs/Ge Solar Cells  
 AlGaAs Window Depth:  $0.08 \mu$   
 Junction Depth:  $0.50 \mu$   
 Buffer Layer:  $6-9 \mu$   
 $2 \times 2 \text{ cm} \times 225 \mu$   
 Dual AR Coating  
 Sample Size 5 TM-91

Cell Temp. ( $^{\circ}\text{C}$ )	Solar Intensity ( $\text{mW/cm}^2$ )			
	<u>50</u>	<u>100</u>	<u>135.3</u>	<u>250</u>
-20	986.0	1049.1	1070.0	1094.4
28	852.3	904.4	923.3	945.9
60	749.4	797.5	817.4	844.1
100	631.7	673.2	689.7	716.5
140	527.2	568.6	586.3	617.4

Table 11. Average Maximum Power: After  $1 \times 10^{16}$  e/cm<sup>2</sup>

ASEC GaAs/Ge Solar Cells  
 AlGaAs Window Depth: 0.08  $\mu$   
 Junction Depth: 0.50  $\mu$   
 Buffer Layer: 6-9  $\mu$   
 2 x 2 cm x 225  $\mu$   
 Dual AR Coating  
 Sample Size 5 TM-91

Cell Temp. ( °C )	Solar Intensity (mW/cm <sup>2</sup> )			
	<u>50</u>	<u>100</u>	<u>135.3</u>	<u>250</u>
-20	15.94	34.61	48.47	89.34
28	14.35	31.09	43.73	81.32
60	12.84	27.79	39.31	72.67
100	11.01	24.24	33.68	62.52
140	9.14	20.46	29.03	55.94

Table 12. Average Fill Factor: After  $1 \times 10^{16}$  e/cm<sup>2</sup>

ASEC GaAs/Ge Solar Cells  
 AlGaAs Window Depth: 0.08  $\mu$   
 Junction Depth: 0.50  $\mu$   
 Buffer Layer: 6-9  $\mu$   
 2 x 2 cm x 225  $\mu$   
 Dual AR Coating  
 Sample Size 5 TM-91

Cell Temp. ( °C )	Solar Intensity (mW/cm <sup>2</sup> )			
	<u>50</u>	<u>100</u>	<u>135.3</u>	<u>250</u>
-20	0.702	0.719	0.724	0.709
28	0.691	0.709	0.715	0.710
60	0.680	0.693	0.696	0.690
100	0.659	0.674	0.675	0.663
140	0.621	0.641	0.648	0.652

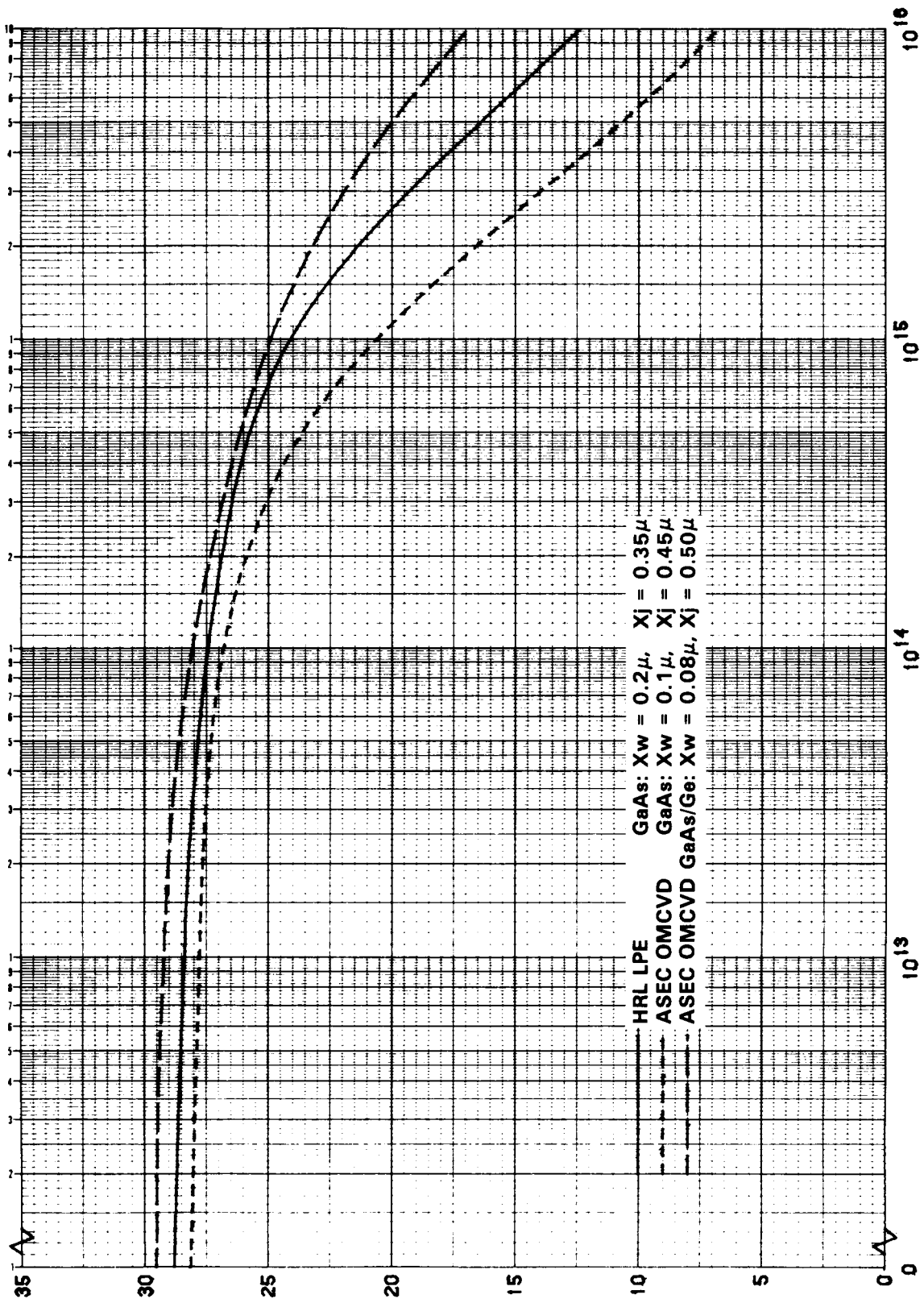


Figure 1.  $I_{sc}$  vs 1 MeV Electron Fluence for Three Types of GaAs Solar Cells

ORIGINAL PAGE IS  
OF POOR QUALITY

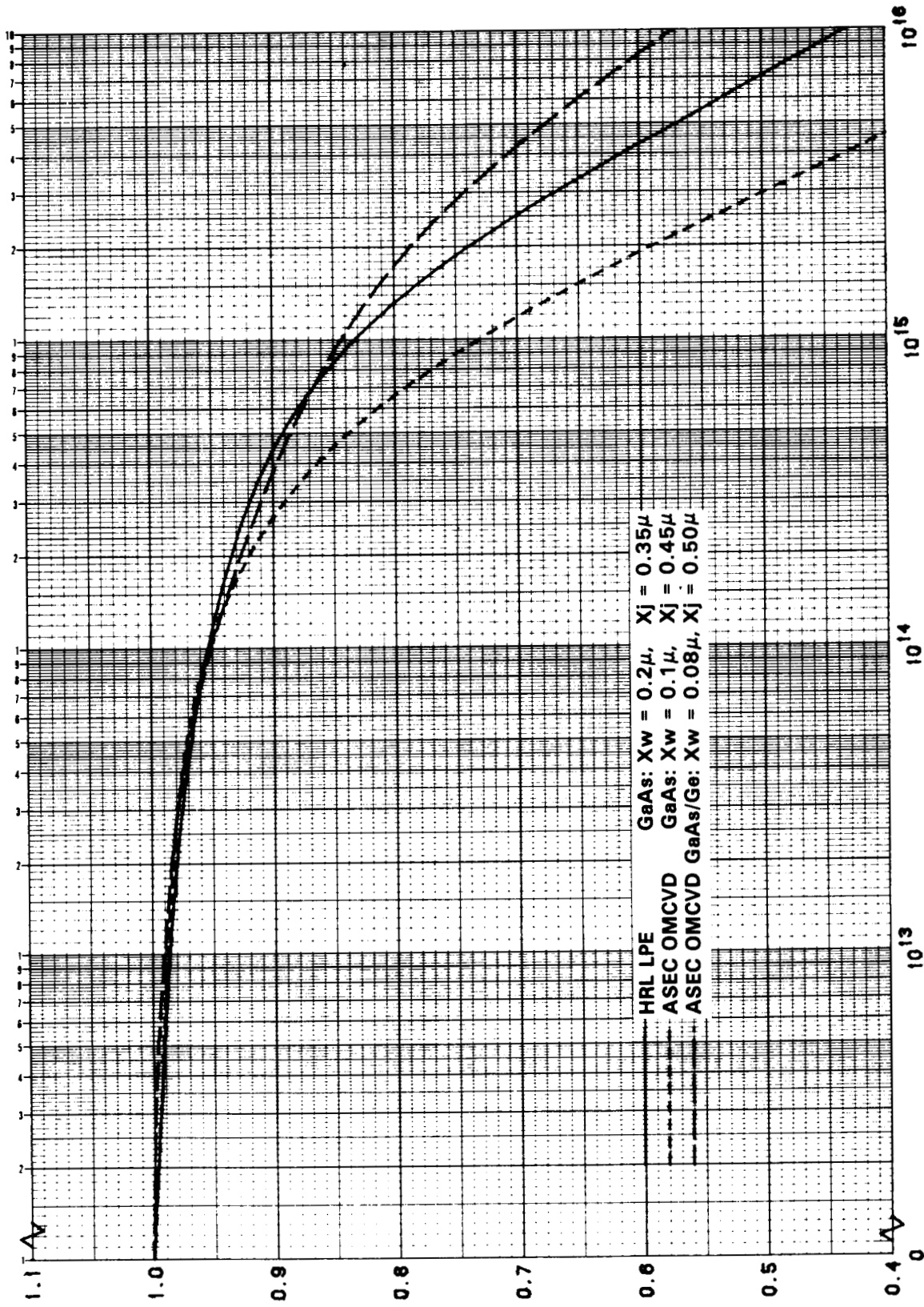


Figure 2. Normalized  $I_{sc}$  vs 1 MeV Electron Fluence for Three Types of GaAs Solar Cells

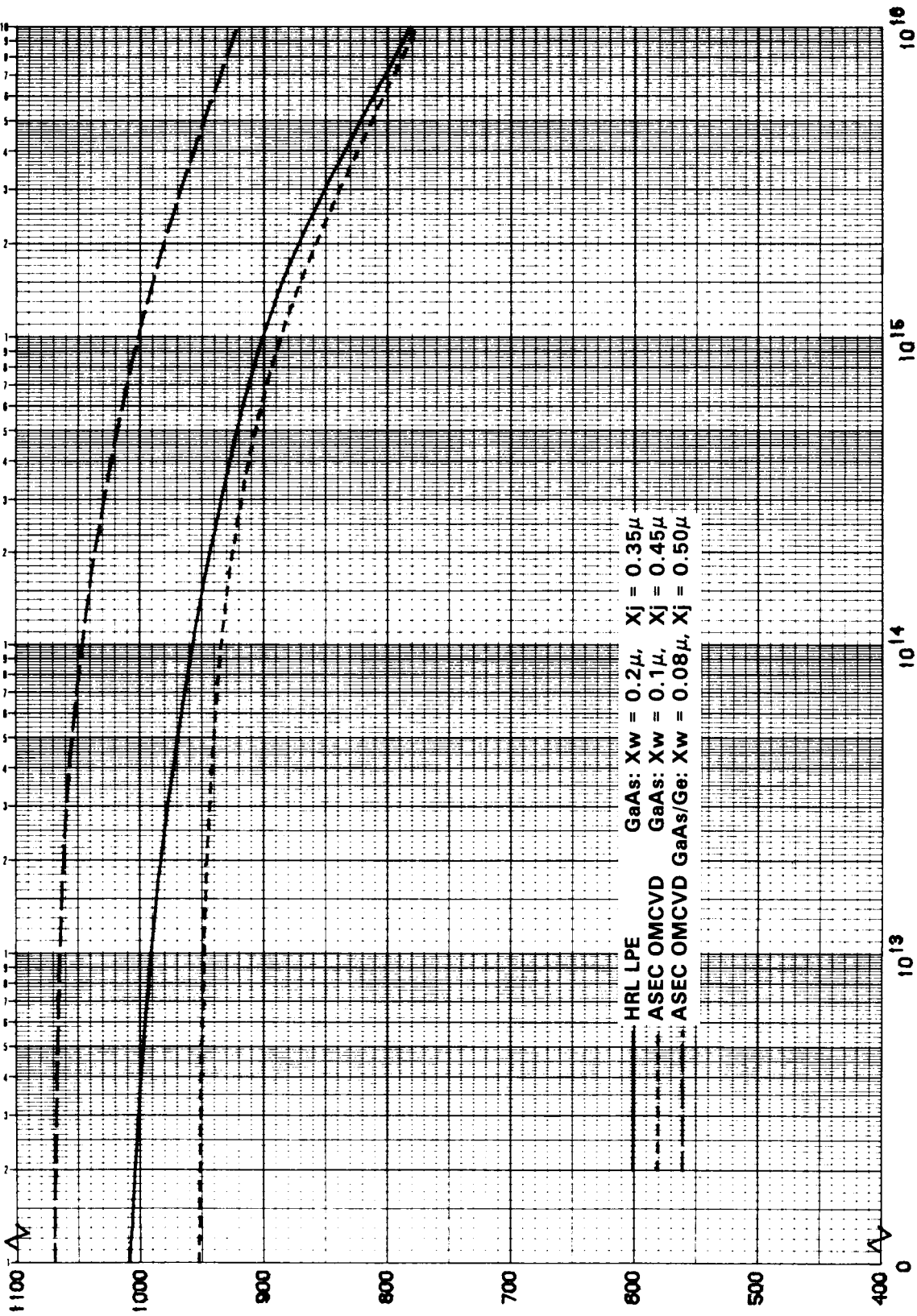


Figure 3.  $V_{oc}$  vs 1 MeV Electron Fluence for Three Types of GaAs Solar Cells

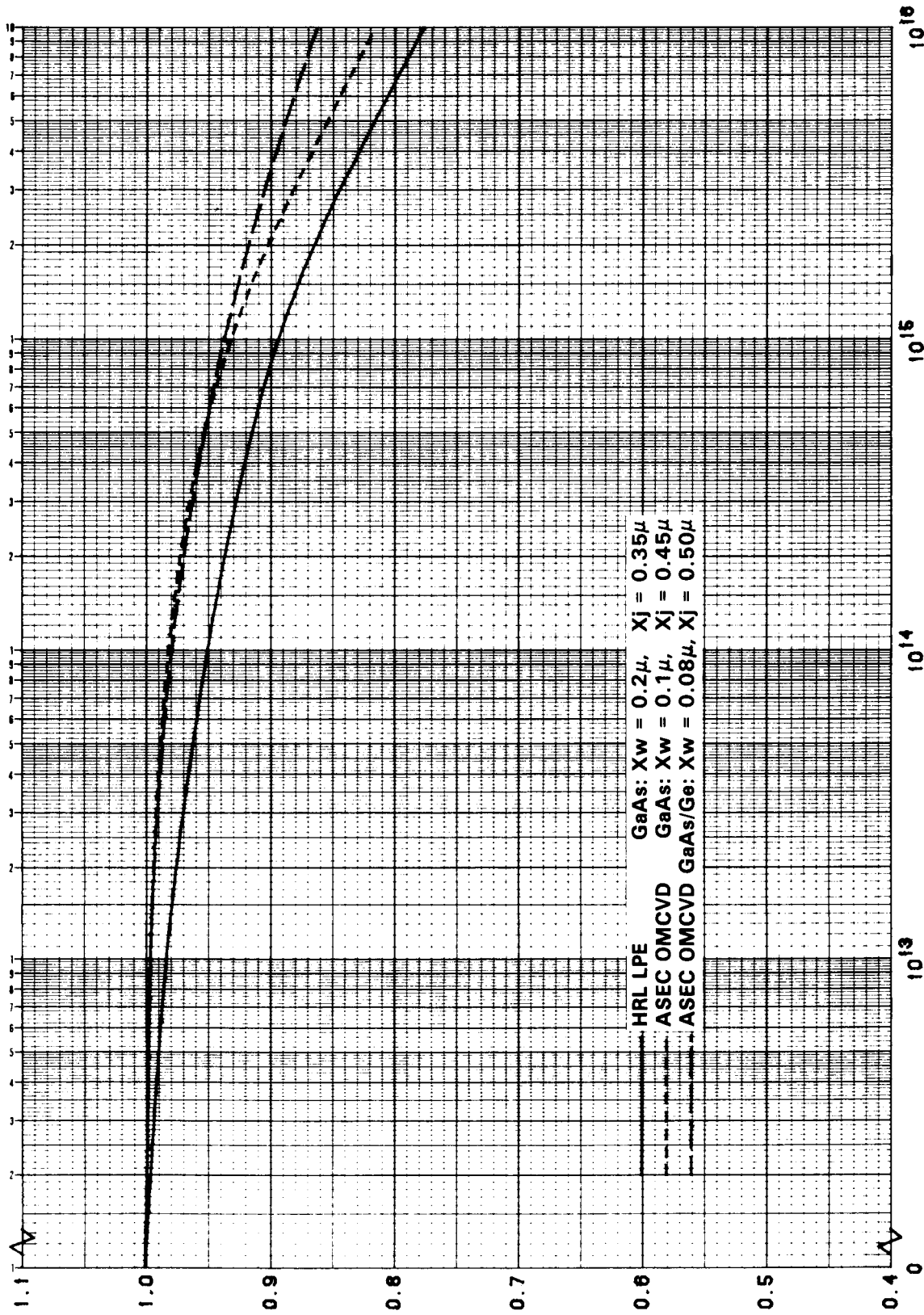


Figure 4. Normalized  $V_{OC}$  vs 1 MeV Electron Fluence for Three Types of GaAs Solar Cells

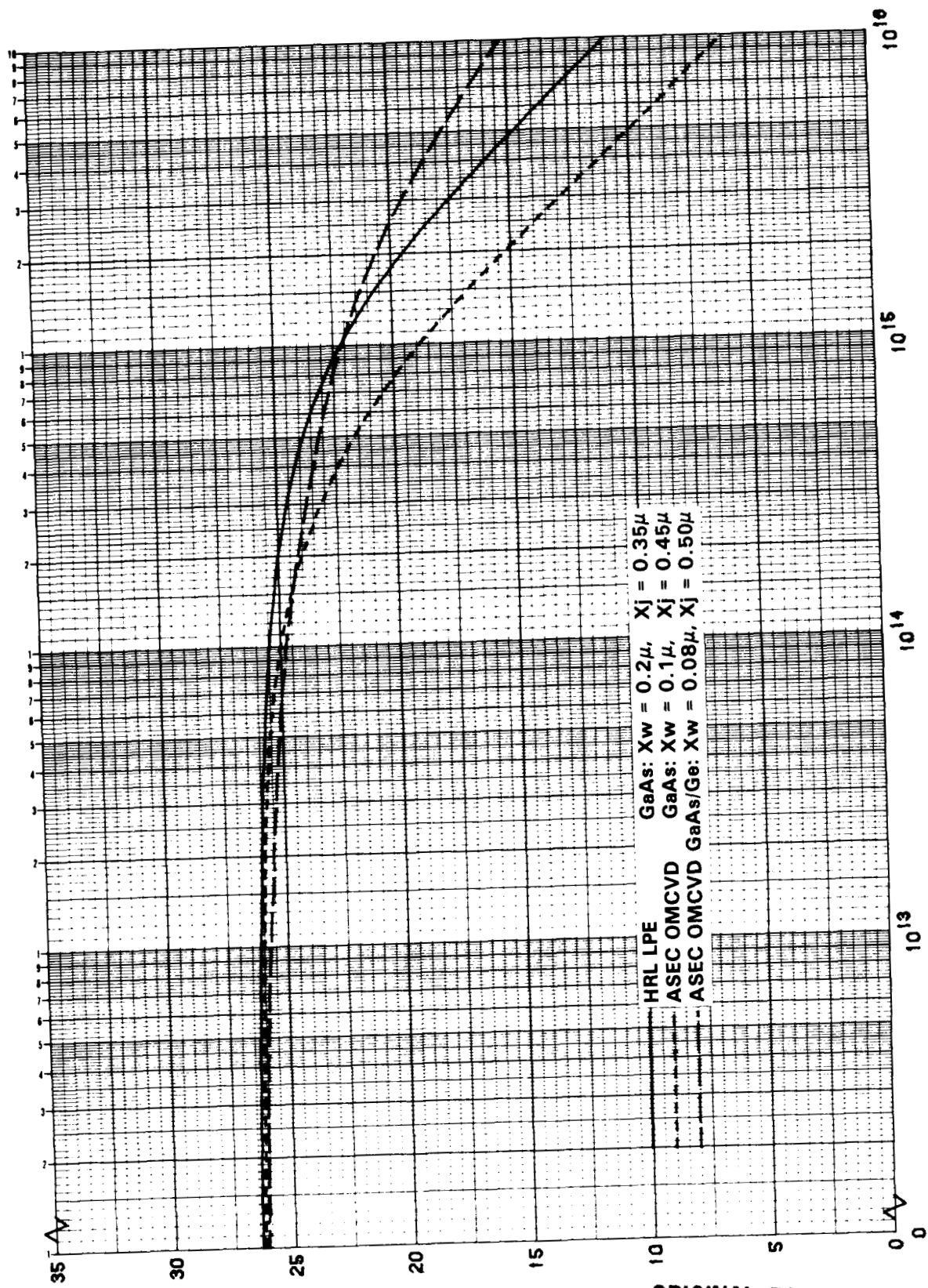


Figure 5.  $I_{mp}$  vs 1 MeV Electron Fluence for Three Types of GaAs Solar Cells

ORIGINAL PAGE IS  
OF POOR QUALITY

ORIGINAL PAGE IS  
OF POOR QUALITY

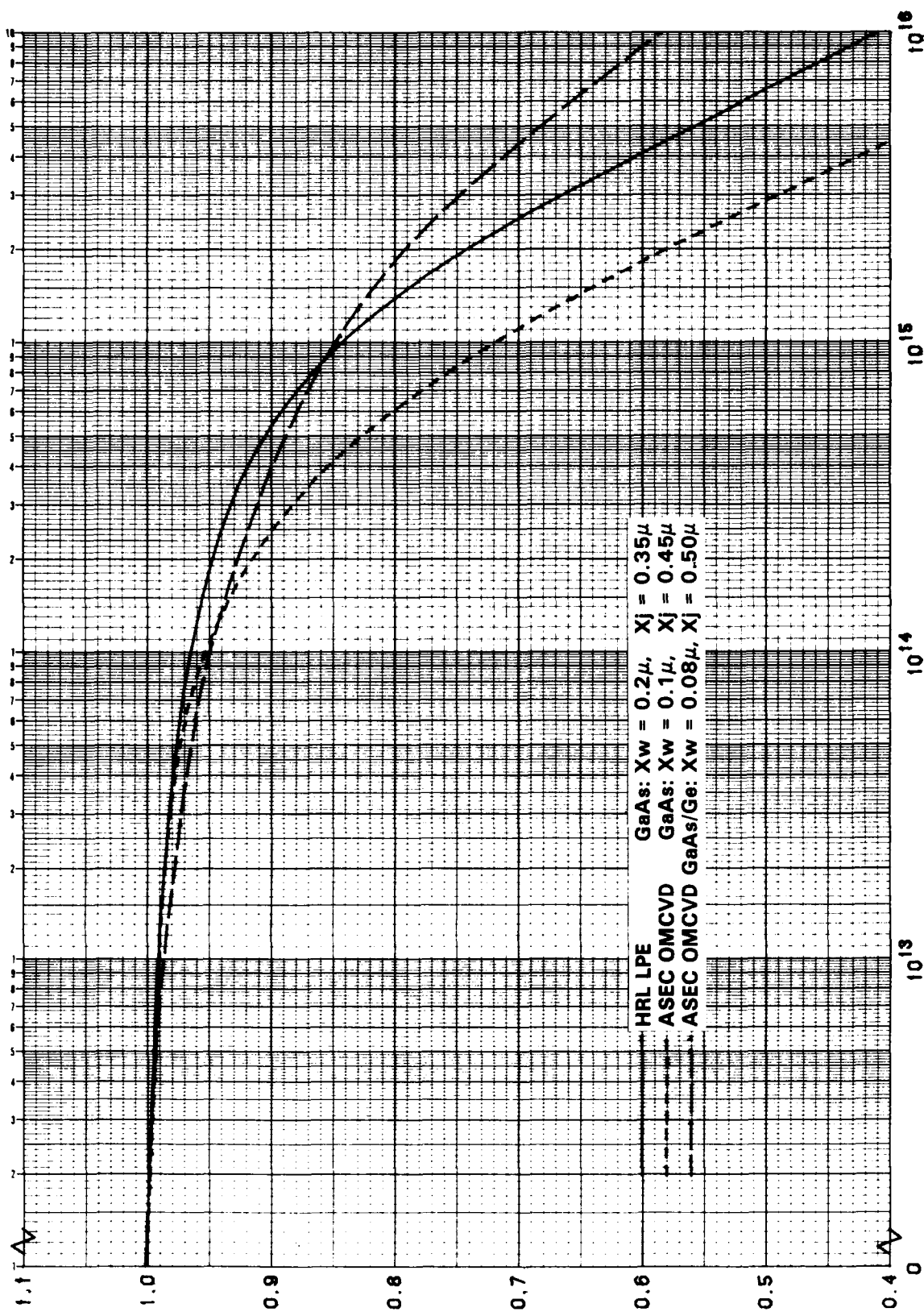


Figure 6. Normalized  $I_{mp}$  vs 1 MeV Electron Fluence for Three Types of GaAs Solar Cells

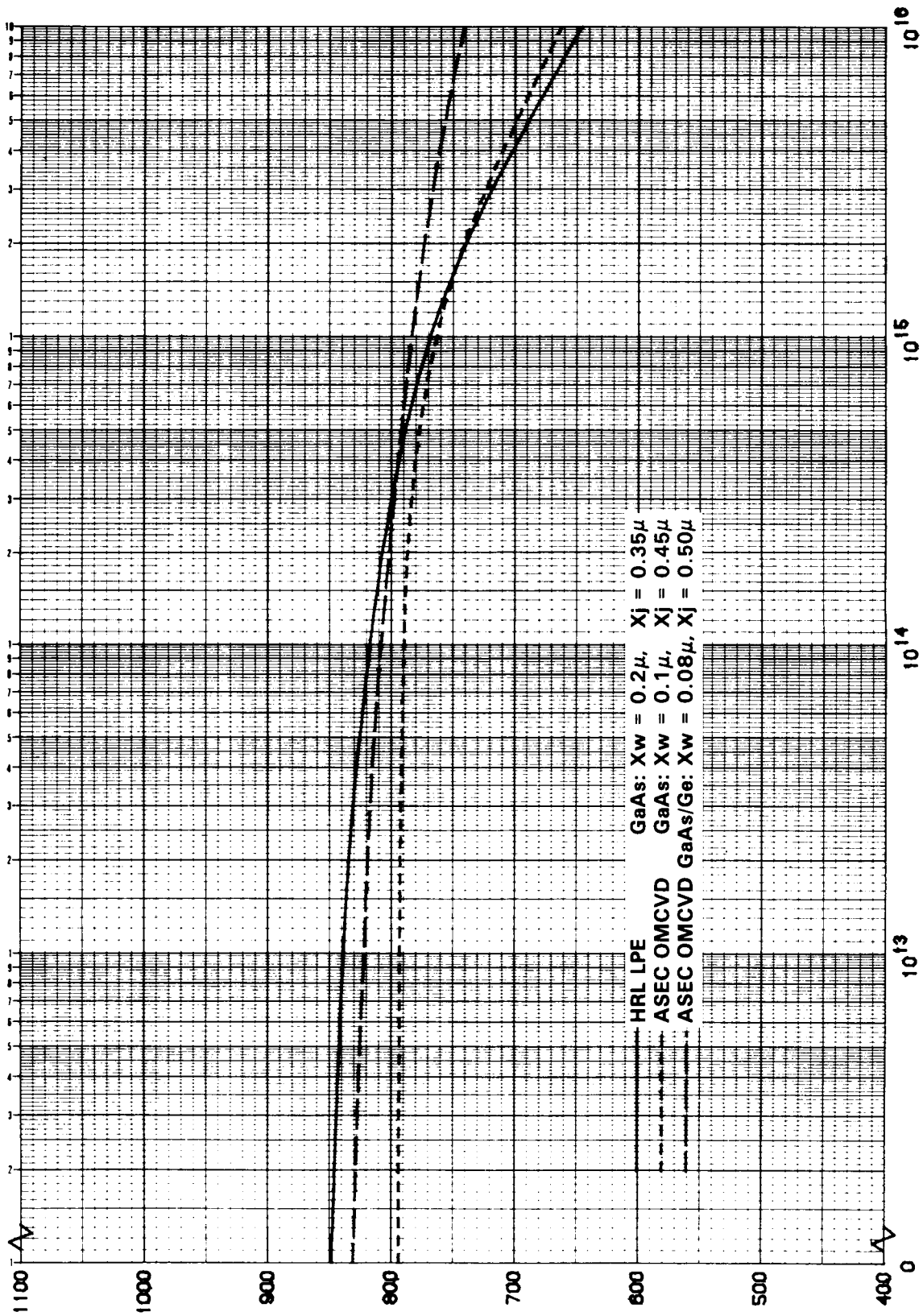


Figure 7.  $V_{mp}$  vs 1 MeV Electron Fluence for Three Types of GaAs Solar Cells



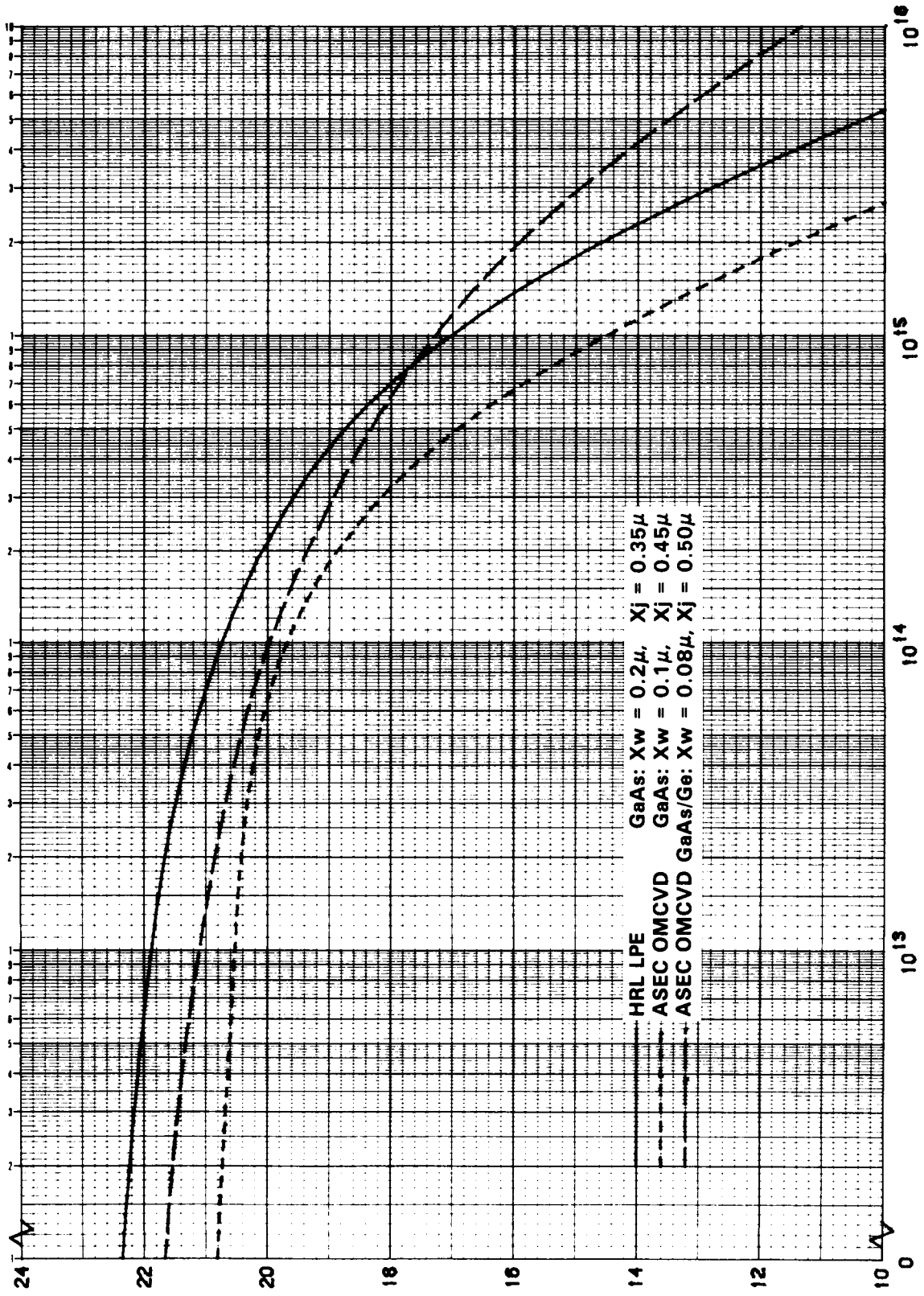


Figure 9.  $P_{max}$  vs 1 MeV Electron Fluence for Three Types of GaAs Solar Cells

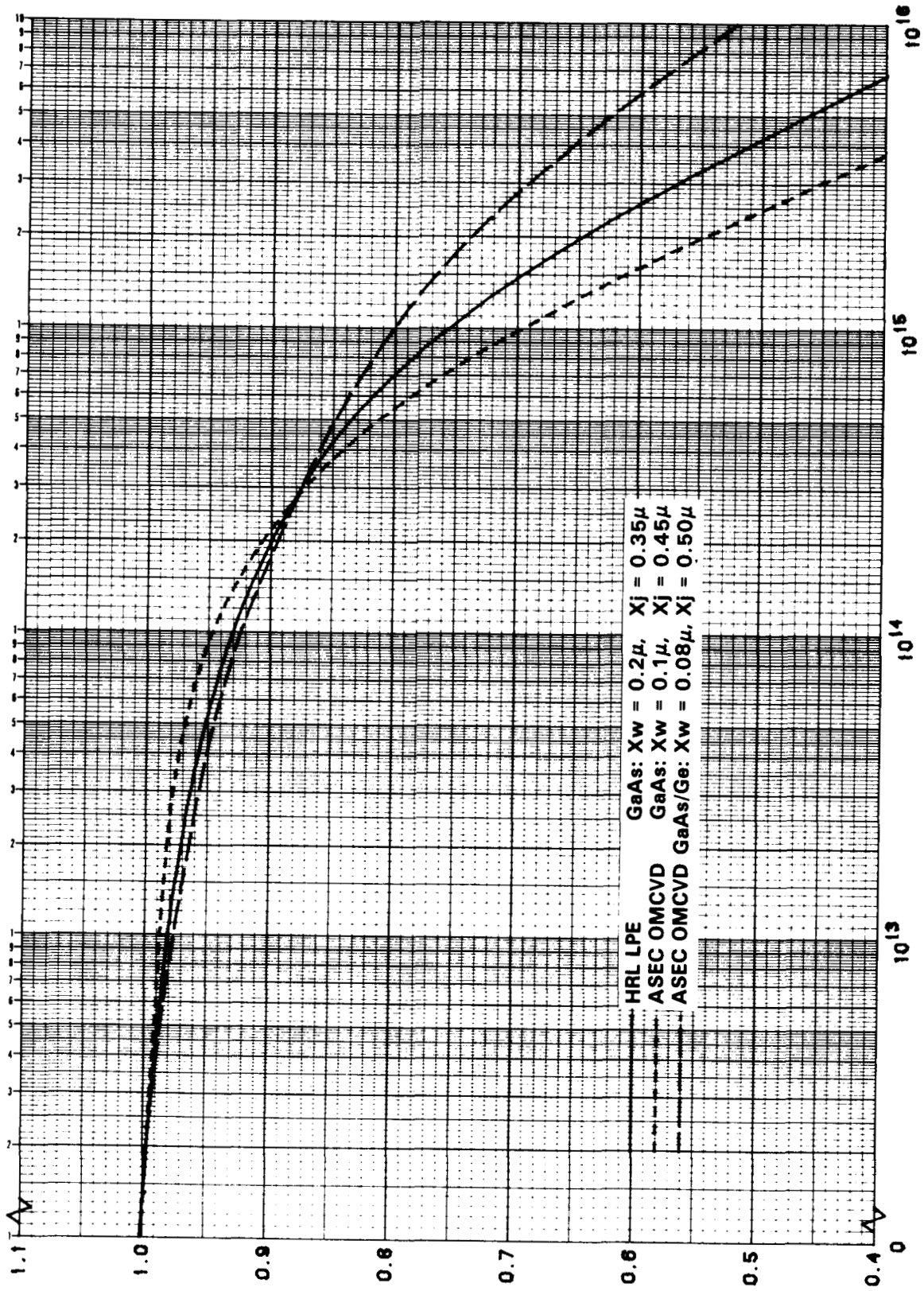


Figure 10. Normalized  $P_{max}$  vs 1 MeV Electron Fluence for Three Types of GaAs Solar Cells

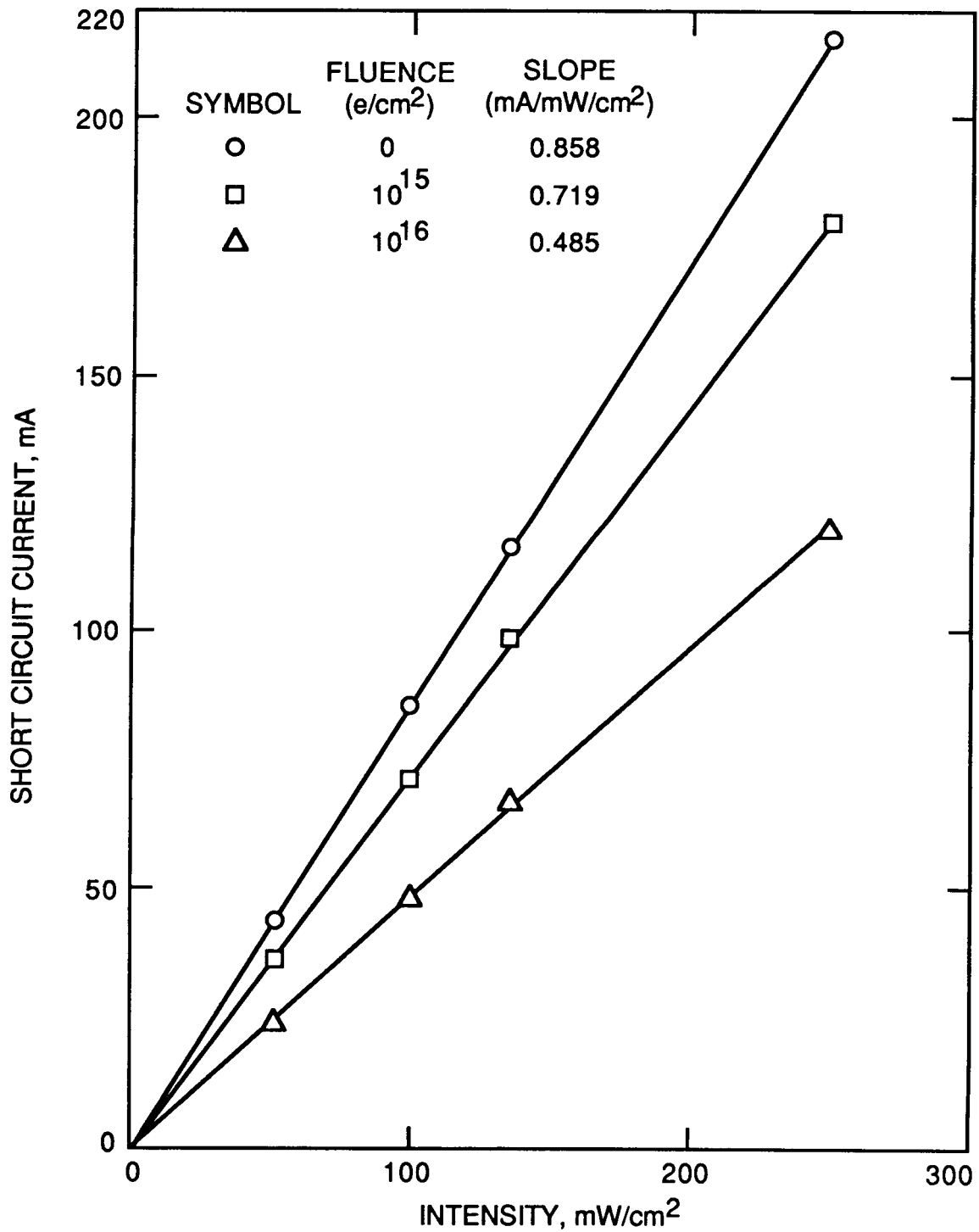


Figure 11.  $I_{sc}$  vs Intensity at 28°C for GaAs/Ge Solar Cells

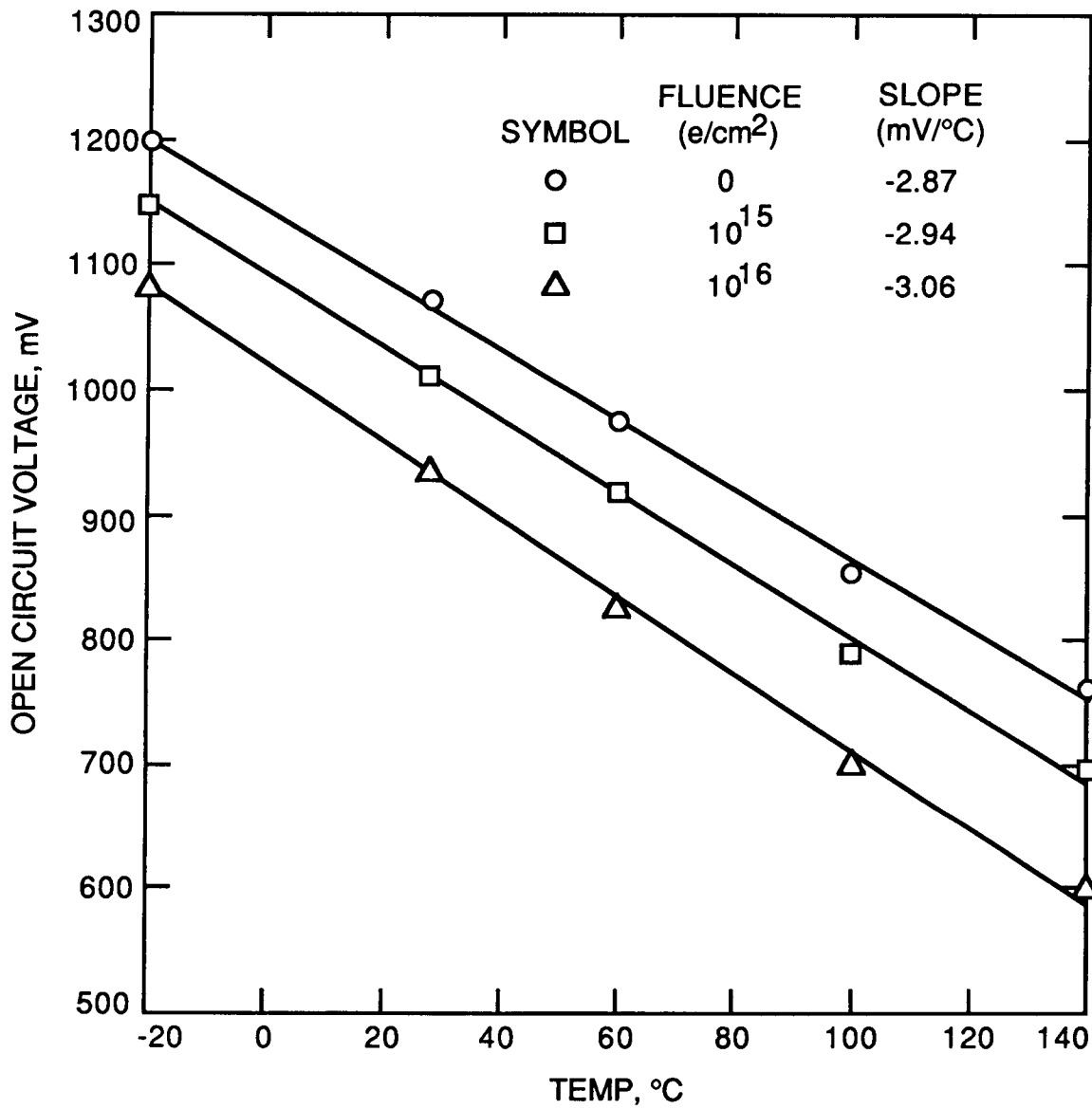


Figure 12.  $V_{OC}$  vs Temperature at  $135.3 \text{ mW/cm}^2$  for GaAs/Ge Solar Cells

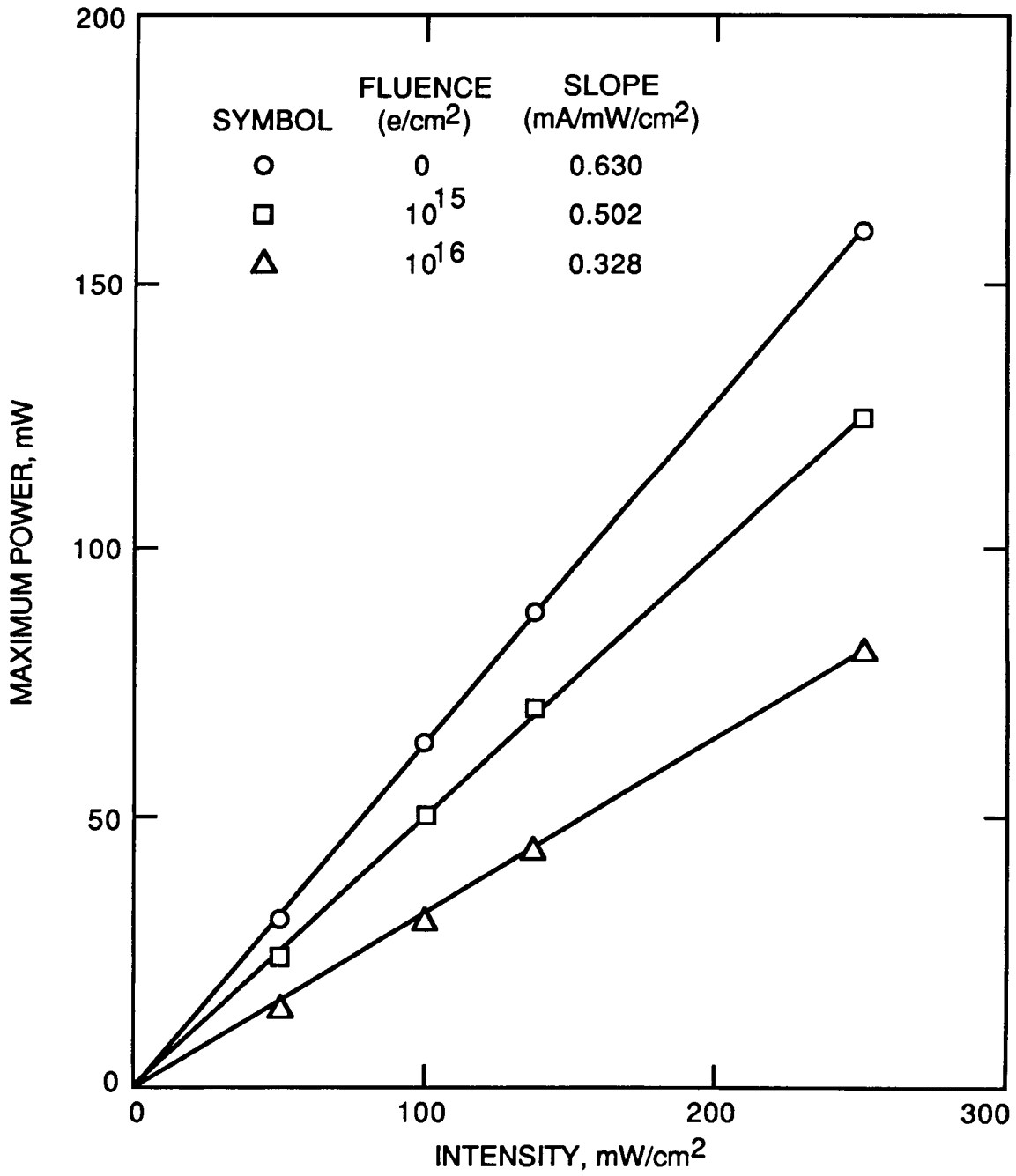


Figure 13.  $P_{max}$  vs Intensity at 28°C for GaAs/Ge Solar Cells

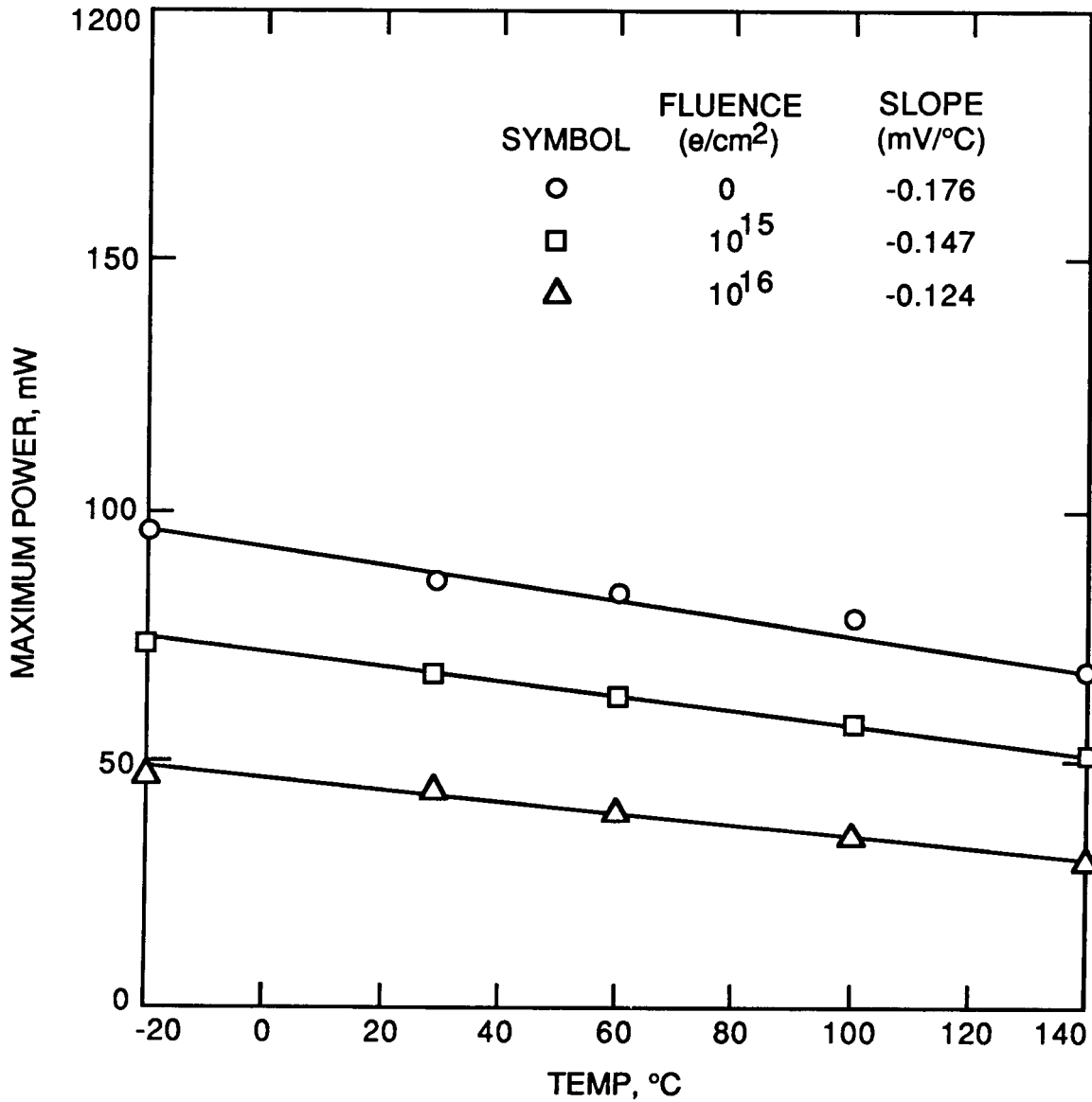


Figure 14.  $P_{max}$  vs Temperature at  $135.3 \text{ mW/cm}^2$  for GaAs/Ge Solar Cells

## APPENDIX

### PHOTON DEGRADATION OF AlGaAs/GaAs SOLAR CELLS

Bruce Anspaugh and Ram Kachare

Jet Propulsion Laboratory  
California Institute of Technology  
Pasadena, California 91109

and

Peter Iles  
Applied Solar Energy Corporation  
15251 E. Don Julian Road  
City of Industry, CA 91746

#### ABSTRACT

More than fifty-five OMCVD AlGaAs/GaAs solar cells were exposed for over 400 hours to AMO photons at 28°C in three separate, well-controlled runs. Significant degradation of solar cell efficiency was observed in two out of the three runs. Though noticeable losses in the open-circuit voltage, fill factor, and maximum power were observed, no change in the short-circuit current was found.

Control cells, mounted beside the test cells, were treated to the same environment except that they were shielded from the light beam. No change was seen in any of the control cells.

In one of the runs, no change was seen in either the test cells or the control cells. Each cell in this run was protected with a coverglass, and was connected to the I-V electrical circuitry through soldered contacts. The cells in this run also had thicker buffer layers and thinner window layers than the cells in the other two runs.

Specific photodegradation mechanisms for the GaAs solar cells are at this time unknown. The detailed results of these experiments are presented.

#### INTRODUCTION

$\text{Al}_x\text{Ga}_{1-x}\text{As}$  windowed GaAs p-n junction solar cells having AMO efficiencies as high as 21% have been fabricated (1) by using an organometallic chemical vapor deposition (OMCVD) growth technique. This approach is now considered as a viable manufacturing process and GaAs solar cells having AMO efficiencies exceeding 17% are routinely produced. These cells have also shown superior radiation hardness compared to that of silicon solar cells and have good potential for space applications (2-4). A considerable amount of information on electron and proton irradiation degradation of GaAs solar cells has been reported

(4-7). However, there have been no published studies on the behavior of GaAs solar cells after photon illumination for a prolonged exposure time. This paper presents preliminary results on photon exposure of GaAs solar cells.

#### EXPERIMENTAL

The p-n GaAs solar cells were fabricated at Applied Solar Energy Corporation using a OMCVD (8,9) growth technique. The cell structure, shown in Figure 1, consisted of an n-GaAs substrate doped with silicon, a Se-doped n-GaAs buffer layer, a Zn-doped p-GaAs emitter layer and a thin ( $<0.1 \mu\text{m}$ ) p- $\text{Al}_{0.85}\text{Ga}_{0.15}\text{As}$  window layer. Each cell has a double layer antireflection coating of  $\text{TiO}_2/\text{Al}_2\text{O}_3$ . Details of the cell structural parameters are shown in Figure 1. In a preliminary experiment prior to the measurements reported here, 40 cells having starting efficiencies between 13% and 17% were exposed to a tungsten light source in an open-circuit condition. During the photon exposure, the cell temperature was held at  $\sim 28^\circ\text{C}$ . Light current-voltage (I-V) characteristics were measured before and after several hours of photon exposure indicated that 25 cells showed some photon-induced degradation in cell efficiencies. Some GaAs solar cells were exposed for over 200 hours to AMO photons using an X-25 solar simulator. A majority of the cells showed some degradation in cell performance in this light source also.

In these preliminary experiments where photon degradation was observed for the first time, we questioned our light I-V measurement setup including the cell measurement test fixture, and the computer controlled power supply, each of which could possibly be the source of cell degradation. These were dealt with by designing and building a special cell fixture which applied very low and repeatable pressures to the cell contacts. The fixture incorporated a protection diode across the test cell to protect against the application of accidental large reverse bias voltage spikes. The computer program was modified to minimize the possibility of application of voltage spikes across the cell at any time during I-V measurements.

After taking into account all plausible sources of the measurement related cell degradation, careful light I-V measurements were made on a few cells that were exposed to AMO photons over 300 hours. These cells also showed some photon degradation.

Two controlled photon exposure runs were made to further study the GaAs solar cell degradation. In the first run, 32 GaAs solar cells were mounted on a water-cooled aluminum target plate. Of these, 16 solar cells were exposed to AMO photons and 16 were shielded from the light by aluminum foil which was taped in place with Farlock aluminum Mystik tape. All cells were treated identically and were mounted on the plate using thermal conducting grease (Apiezon H). The cells were manufactured by Applied Solar Energy Corp. (ASEC) under the Air Force Mantech Program. They were 2cm x 2cm and had approximately 4.0  $\mu\text{m}$ -thick buffer layers and 0.1  $\mu\text{m}$ -thick  $\text{Al}_{0.88}\text{Ga}_{0.12}\text{As}$  window layers. The cells were exposed to the X-25 beam for 407 hours at 28°C. The cells were removed from the plate and their light I-V curves were measured. All of the 16 photon-exposed solar cells showed degradation ranging from severe to minor, while none of those in the dark degraded. The light I-V curves of all the exposed cells are shown in Figure 2. Prior to photon exposure, all cells had I-V curves similar to the top curves in the Figure. It is apparent from these curves that there is a wide variation in the amount of degradation experienced by the exposed cells. The light I-V curves of all cells held in the dark were highly reproducible. All degraded cells showed a loss in fill factor (FF), and maximum power ( $P_{\text{max}}$ ). In a few cases there were open-circuit voltage ( $V_{\text{oc}}$ ) losses. Interestingly, none of the degraded cells showed a loss in short-circuit current ( $I_{\text{sc}}$ ).

In a second run, an additional 32 GaAs cells of a different type were exposed in the manner described above: 16 solar cells were exposed to AMO photons and 16 were held in the dark. These cells, measuring 2cm x 4cm, were manufactured in a tightly controlled production run. They had approximately 5  $\mu\text{m}$ -thick n-GaAs buffer layers and 0.08  $\mu\text{m}$ -thick  $\text{Al}_{0.86}\text{Ga}_{0.14}\text{As}$  window layers. These cells were screened by reverse bias stressing using 40 mA reverse bias current. These cells were exposed for 432 hours at 28°C, removed from the plate, and remeasured as discussed before. Seven out of 16 photon-exposed cells showed noticeable degradation (nine did not), while the light I-V curves of all 16 shaded cells repeated their pre-exposure curves exactly. The light I-V curves of all the exposed cells for this run are shown in Figure 3.

A third additional controlled photon exposure run was made using 15 current production GaAs cells from ASEC. These 15 cells, each of 2cm x 4cm area, had 6  $\mu\text{m}$ -thick n-GaAs buffer layers and 0.05  $\mu\text{m}$   $\text{Al}_{0.85}\text{Ga}_{0.15}\text{As}$  window layers. They were also screened by the reverse bias stress described above. However, each of these cells was fitted with a coverglass (for practical purposes, it is extremely unlikely that any solar cells will be flown without coverglasses) and was mounted on the aluminum exposure plate using Apiezon H grease and permanent hardwired connections. The hardwired

connections allowed the measurement of light I-V curves without removing the cells from the plate or placement into and removal from a fixture. In this run, 12 of the 15 cells were exposed to the light beam and 3 were kept in the dark using a quickly removable shadow plate. Light I-V curves were measured several times during the 552 hour exposure. The light I-V curves for all the exposed cells are shown in Figure 4. As can be seen from the figure, none of the exposed cells in this run showed any degradation. As in the previous runs, the shielded cells did not degrade in this run either. Table 1 gives a summary of the properties of all cells used in the three controlled runs.

## RESULTS

In the first controlled run, the most severely degraded cell showed decreases in  $P_{\text{max}}$  from 92.0 mW to 84.0 mW after exposure,  $V_{\text{oc}}$  from 993 to 986 mV, FF from 0.81 to 0.74, and no decrease in  $I_{\text{sc}}$ . The exposed cell which degraded the least showed decreases in these parameters as follows:  $P_{\text{max}}$  from 92.5 to 92.0 mW,  $V_{\text{oc}}$  from 990 to 983 mV, and FF from 0.80 to 0.79.

In the second run, the most photon degraded cell showed losses in  $P_{\text{max}}$  from 194.3 to 143.7 mW,  $V_{\text{oc}}$  from 1015 to 984 mV, and FF from 0.80 to 0.61. The exposed cell which showed the lowest degradation had changes in  $P_{\text{max}}$  from 204 to 196.5 mW,  $V_{\text{oc}}$  from 1005 to 1002 mV, and FF from 0.81 to 0.79. As stated before no loss in  $I_{\text{sc}}$  was observed for any cell, exposed or unexposed, in these experiments.

## DISCUSSION

Plausible causes of the photon degradation in two runs and no degradation in the third run need careful consideration. Since there is no degradation in  $I_{\text{sc}}$ , the photons that are degrading  $V_{\text{oc}}$ ,  $P_{\text{max}}$ , and FF are, most probably, not producing highly electrically active defects; that is, the minority carrier lifetime is not degraded. The loss in  $V_{\text{oc}}$  and FF could either be related to p- or n- metal contact reactions with GaAs or with an inherent internal device degradation process of an unknown nature. It is hard to believe that photons alone at about 28°C can degrade the metal contacts, either by photochemical reaction between metal and GaAs or electrochemical as well as thermal migration of metals into the active regions of the cells. However, we do not rule out the possibility of inducing some dislocations in the vicinity of the metal-GaAs interface either during metallization or by contact probes during measurements of the light I-V curves. It is well known (10) that dislocations can be introduced in GaAs by applying excessive pressure. Dislocation loops (10) are generated after scratching the GaAs surface. If the contact probes were responsible for the cell degradation, then some degradation would have been observed on the shaded cells.

Since all photon exposed cells did not degrade in two of the runs, it could be speculated that the cells which showed degradation might be containing OMCVD growth or metallization-related defects which get activated during the photon exposure. The

factors that are important in the dynamics of dislocations (10-12) are: (a) interaction of point defects with dislocations, particularly at the AlGaAs/GaAs interface, (b) stress/strain at the metal-GaAs interface, and (c) different optoelectronic properties of interfaces and defects.

Recently photon-induced degradation of amorphous silicon solar cells has been explained (13) by using a defect reaction process that is induced by the energy release during electron-hole (e-h) recombination. One could postulate that the e-h recombination assists diffusion of defects from the metal-GaAs (top p-GaAs layer) interface into the active area of the cell and consequently degrades the GaAs solar cell.

The fact that  $I_{sc}$  does not change after photon exposure is a very important experimental observation. Recently, the effect of dislocations in metal-insulator silicon solar cells was explained by a model based on hopping conduction of capture carriers along dislocations (14). In these cells, dislocations of different lengths were intentionally introduced by polishing silicon wafers with  $Al_2O_3$  powder of different grits. The light I-V curves of these cells showed losses in  $P_{max}$ ,  $V_{oc}$ , and FF, but not in  $I_{sc}$  when dislocation lengths were increased. If conduction and shunting are the important roles of dislocations, then, as shown by the model calculations (14),  $I_{sc}$  is unaffected while  $V_{oc}$  is strongly decreased. This constitutes a piece of compelling evidence in favor of conduction along the dislocations in GaAs. Unfortunately, at present, the conductivity data on dislocations in GaAs is not available.

In our third photon exposure run, we did not observe photo-degradation even in a single cell. These cells are from a current production process. Differences in the properties of these cells compared to those cells used in the other two runs are shown in Table 1. As can be seen, each cell in the third run has a thick n-GaAs buffer layer, a very thin AlGaAs window layer, protection by a coverglass, and is hardwired to avoid direct probing of the cell contacts during light I-V measurements. At present, whether growth process, layer thicknesses, coverglass, or hardwiring has played any role in eliminating the photon degradation effect is unknown. Possible prevention of degradation by the hardwiring is less likely, since shaded cells subjected to repeated testing did not show any degradation. Assuming that the coverglass plays a predominant role, the loss mechanism is likely to be related to interaction by energetic UV photons. For surface dominated devices like GaAs cells, this could perhaps affect either the passivated region at the heteroface, or the shallow emitter properties. It is clear that additional experiments need to be performed to find out what property or properties of cells used in the first two runs contributed to the observed photon degradation.

## CONCLUSIONS

[1]. Three well controlled photon exposure runs were made on OMCVD GaAs solar cells. Two runs showed some degree of photon degradation.

[2]. Not all cells in the two runs degraded equally. Some photon exposed cells did not degrade at all.

[3]. Losses in  $P_{max}$ ,  $V_{oc}$ , and FF were observed in photon degraded cells. However, no loss in  $I_{sc}$  was observed.

[4]. One run showed no degradation.

[5]. A plausible cause of the photon-degradation is presently not known. However, several speculative degradation mechanisms were discussed.

[6]. Additional photon exposure experiments need to be performed to identify the cause and indicate a cure for photon degradation in GaAs solar cells. Future tests must explain the cure demonstrated in the third run, and must relate this cure to plausible causes for the degradation.

## ACKNOWLEDGEMENT

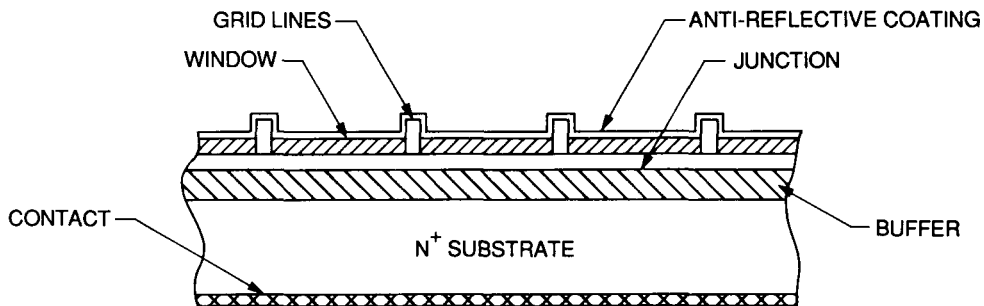
The research described in this paper was carried out by the Jet Propulsion Laboratory, California Institute of Technology, and was sponsored by the U.S. Air Force Wright Aeronautical Laboratory and the National Aeronautics and Space Administration.

## REFERENCES

1. J. G. Werthen, G. F. Virshup, C. W. Ford, C. R. Lewis, and H. C. Hamaker, *Appl. Phys. Letters*, **48**, 74, 1986.
2. M. Yamaguchi and C. Amaro, *J. Appl. Phys.*, **57**, 537, 1987.
3. R. Loo, R. C. Knechtli, and G. S. Kamath, *Conf. Record of the 15th IEEE Photovoltaic Specialists Conf.*, 33, 1981.
4. B. E. Anspaugh and R. G. Downing, *Conf. Record of the 17th IEEE Photovoltaic Specialists Conf.*, 23, 1984.
5. M. Yamaguchi and C. Amano, *J. Appl. Phys.*, **54**, 5021, 1983.
6. S. Yoshida, K. Mitsui, T. Oda, and Y. Yukimoto, *Japanese J. Appl. Phys.*, **21**, Suppl. 2, 27, 1982.
7. S. S. Li, T. T. Chu, and R. Loo, *IEEE Trans. Nucl. Sci.*, **NS-28**, No. 6, 4113, 1981.
8. T. Nakarisi, *J. Cryst. Growth*, **68**, 282, 1984.
9. J. Van de Ven, H. G. Shoot, and L. J. Giling, *J. Appl. Phys.*, **60**, 1684, 1986.
10. K. H. Knester, B. C. DeCooman, and C. B. Carter, *J. Appl. Phys.*, **58**, 4065, 1985.
11. P. W. Hutchinson, P. S. Dobsen, S. O'Hara, and D. H. Newman, *Appl. Phys. Letters*, **26**, 250, 1975.
12. P. Petroff, W. D. Johnston, and R. L. Hartman, *Appl. Phys. Letters*, **25**, 226, 1974.
13. D. Redfield, *Appl. Phys. Letters*, **48**, 846, 1986.
14. W. M. Ranjith Divigalpitiya, and S. Roy Morrison, *J. Appl. Phys.*, **60**, 406, 1986.

Table 1. Properties of GaAs Cells Used in Photon Exposure Tests

PROPERTY	MANTECH	LIMITED CUSTOM RUN	CURRENT PRODUCTION
RUN NO.	1	2	3
AlGaAs Substrate	Si doped, $2 \times 10^{18}$ , 12 mil	Si doped, $2 \times 10^{18}$ , 12 mil	Si doped, $2 \times 10^{18}$ , 12 mil
n-GaAs Buffer	Se doped, $2 \times 10^{17}$ , 4 $\mu\text{m}$	Se doped, $2 \times 10^{17}$ , 5 $\mu\text{m}$	Se doped, $2 \times 10^{17}$ , 6 $\mu\text{m}$
p-GaAs Emitter	Zn doped, $1 \times 10^{18}$ , $\sim 0.5 \mu\text{m}$	Zn doped, $1 \times 10^{18}$ , 0.7 $\mu\text{m}$	Zn doped, $1 \times 10^{18}$ , $\sim 0.5 \mu\text{m}$
p-AlGaAs Window x value	Zn doped, $1 \times 10^{18}$ , 0.1 $\mu\text{m}$ 0.88 (+ in some cases)	Zn doped, $1 \times 10^{18}$ , 0.08 $\mu\text{m}$ 0.85 - 0.87	Zn doped, $1 \times 10^{18}$ , 0.05 $\mu\text{m}$ 0.85 - 0.87
Front Contacts	AuZnAuAg, $\geq 4 \mu\text{m}$	AuZnAuAg, $\geq 4 \mu\text{m}$	AuZnAuAg, $\geq 4 \mu\text{m}$
Back Contacts	AuGeNiAg, $\geq 4 \mu\text{m}$	AuGeNiAg, $\geq 4 \mu\text{m}$	AuGeNiAg, $\geq 4 \mu\text{m}$
AR Coating	Dual	Dual	Dual
Reverse Bias Screening	No	Yes	Yes
Coverglass	No	No	Yes
Hardwired	No	No	Yes
Soldered	No	Zone-soldered	Zone-soldered
Light Source	X-25, 135.3 mW/cm <sup>2</sup>	X-25, 135.3 mW/cm <sup>2</sup>	X-25, 135.3 mW/cm <sup>2</sup>
Average Temp. During Exposure	$\leq 28^\circ\text{C}$	$\leq 28^\circ\text{C}$	$\leq 28^\circ\text{C}$
Sample Size			
Exposed	16	16	12
Shielded	16	16	3
Photon Exposure Time	407 hours	432 hours	552 hours



ELEMENT	THICKNESS ( $\mu\text{m}$ )	COMPOSITION	DOPANT CONCENTRATION $\times 10^{18} \text{ cm}^{-3}$
GRID (p-CONTACT)	3.4	Ag - Au Zn Au	-
AR COATING	0.1	Ti O <sub>x</sub> /Al <sub>2</sub> O <sub>3</sub>	-
WINDOW (p <sup>+</sup> )	0.1	Al <sub>x</sub> Ga <sub>1-x</sub> As (Zn)	2 TO 4
JUNCTION (p)	0.45	GaAs (Zn)	2
BUFFER (n)	10	GaAs (Se)	0.2 TO 0.5
SUBSTRATE (n <sup>+</sup> )	355	GaAs (Si DOPANT)	1 TO 4
n - CONTACT	3.4	Ag - Au Ge Ni Au	-

Figure 1. Schematic of Gallium Arsenide Cell Structure

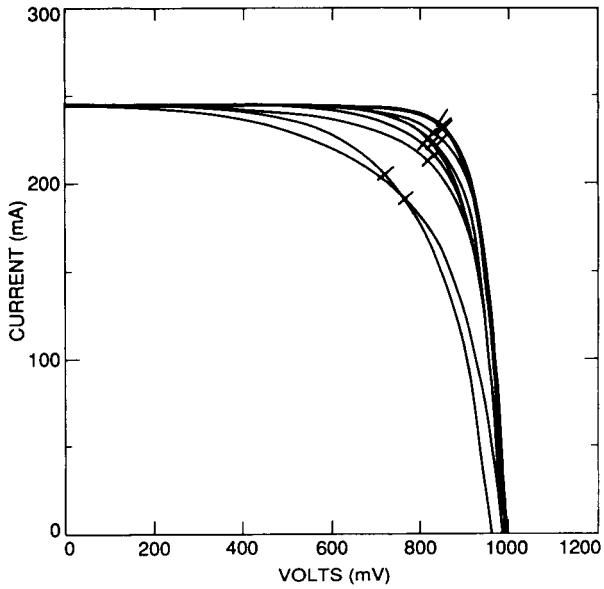


Figure 2. Light I-V Curves of Mantech GaAs Cells After 407 hour Photon Exposure

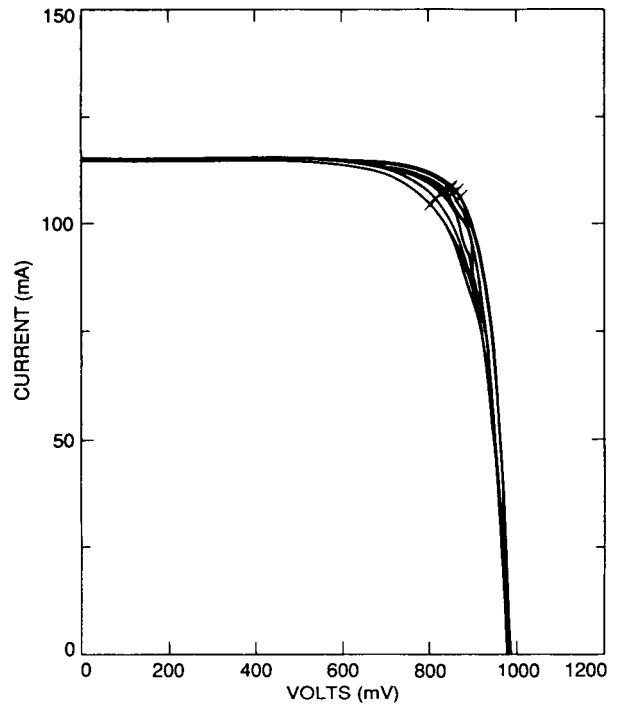


Figure 3. Light I-V Curves of Custom Run GaAs Cells After 432 hour Photon Exposure

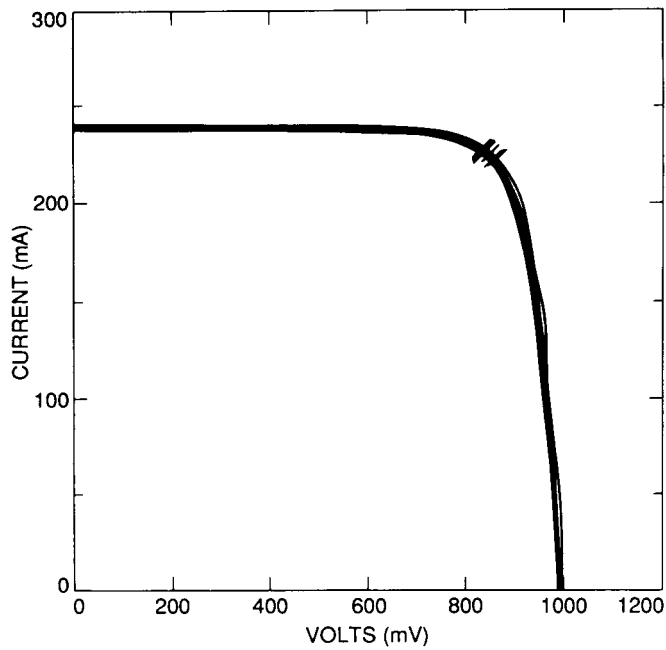


Figure 4. Light I-V Curves of Current Production GaAs Cells After 552 hours Photon Exposure